

Fabrication and Characterization of Al5083/Al₂O₃ Surface Nanocomposite via Friction Stir Processing

Akbar Heidarpour^{1,*}, Saeed Ahmadifard², Shahab Kazemi²

¹ Department of Metallurgy and Materials Engineering, Hamedan University of Technology, Hamedan, Iran

² Department of Material Engineering, Bu Ali Sina University, Hamedan, Iran

ARTICLE INFO

Article history:

Received 16 November 2016

Accepted 7 January 2017

Available online 25 June 2017

Keywords:

Friction stir processing

Nanocomposite

Microhardness

Grain refinement

Wear

ABSTRACT

In the present study, Al5083- Al₂O₃ nanocomposite was successfully prepared by friction stir processing (FSP) with the rotational speed of 710 rpm and travel speed of 14 mm/min. In order to improve the distribution of Al₂O₃ particles, a net of holes was designed on the surface of Al5083 sheet. The samples were characterized by optical (OM) and scanning electron microscopy (SEM), and microhardness, tensile, and wear tests. The results showed that FSP is an effective process to fabricate Al5083- Al₂O₃ surface nanocomposite. Microstructural observation demonstrated fine and equiaxed grains and homogenous distribution of Al₂O₃ nanoparticles in the stir zone (SZ). The presence of Al₂O₃ nanoparticles leads to a decrease in the grain size from 45 to 7 μm and an increase in microhardness from 80 to 140 Hv and tensile strength from 280 to 335 MPa. Wear test results showed an improvement in wear resistance due to its higher hardness. Also, the wear mechanism in all samples was abrasive.

1-Introduction

Aluminum and its alloys, including Al5083, have low densities, high corrosion resistance, and high strength to weight ratio, which makes them ideal to be extensively used in marine, armor plate, and transportation industries [1]. For many applications, the useful life of components often depends on their surface properties such as wear resistance. In the recent years, much attention has been paid to friction stir processing (FSP) as a surface modification technique [2]. FSP is based on the friction stir welding (FSW) technique invented by TWI in 1991 [2, 3]. In this technique, a rotating tool with a specially designed pin and shoulder enters a monolithic metallic substrate and traverses along the desired path on the surface

of the substrate. Fig. 1 shows a schematic of the FSP experiment. The frictional heating and severe plastic deformation imposed by the rotating tool result in a significant evolution in the local microstructure that is composed of three distinct zones, namely: the heat affected zone (HAZ), the thermomechanically affected zone (TMAZ), and the stir zone (SZ). The most intense plastic deformation and high temperature is experienced by SZ and due to dynamic recrystallization, the grain refinement is achievable there [4, 5]. Furthermore, by incorporating reinforcing particles into the surface, FSP can be used to produce surface composite. It is believed that FSP can improve and modify various characteristics such as yield and tensile properties [6-7], fatigue [8, 9], wear

* Corresponding author:

E-mail address: a.heidarpour@gmail.com

and hardness [10, 11], and corrosion resistance [12].

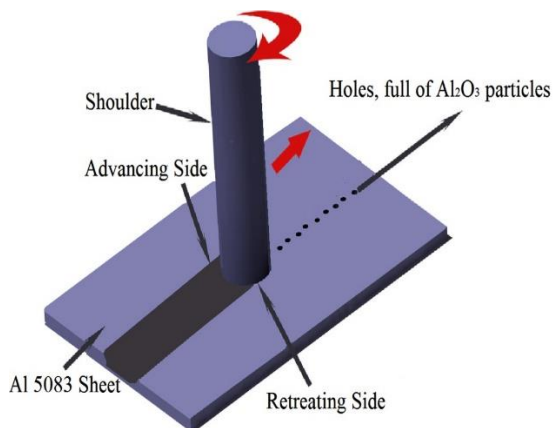


Fig. 1. A schematic view of friction stir processing (FSP) to fabricate Al5083/Al₂O₃ nanocomposite.

Metal matrix composites combine a tough metallic matrix with a hard ceramic reinforcement to produce composite materials with higher mechanical properties than conventional metallic alloys [13, 14]. Some investigations have focused on the formation of MMCs by means of FSP. Hsu et al. [15] achieved an ultrafine-grained Al–Al₂Cu composite by FSP, which benefits from a high Young's modulus, good compressive strength, and reasonably good compressive ductility. Mazaheri et al. [16] also used coating and FSP to fabricate the A356/Al₂O₃ surface composites. In their study, the A356 chips and Al₂O₃ powder particles were mixed and deposited onto grit blasted A356-T6 plates by high velocity oxy-fuel (HVOF) spraying. Subsequently, the plates with composite coatings were subjected to FSP. Hodder et al. [17] coupled cold spraying and FSP to fabricate surface composites. Soleymani et al. [12] fabricated Al5083 / (SiC + MoS₂) via FSP and proved that using a mixture of different powders

results in a better wear behavior. Akramifard et al. [18] used two arrays of drilled holes in fabricating SiC/Cu surface composites with reduced agglomerates of SiC particles. A uniform distribution of reinforcement particles in SZ was observed due to the use of holes.

In this research, Al5083 was used as the base metal and Al₂O₃ as the reinforcing particles. To decrease agglomeration of Al₂O₃ particles, a net of fine holes, instead of grooves, was designed on the surface of Al5083 sheets. Then, microstructural and mechanical properties as well as wear behavior of Al5083 sheets after FSP was investigated.

2- Experimental

The sheet used for the FSP experiments was 5083 aluminum alloy of 5 mm thickness. Chemical composition of aluminum is given in Table 1. The sheet was cut as rectangular samples of 50 mm in width and 150 mm in length. Commercial Al₂O₃ nanoparticles (supplied by the TECNON S.L. Company) of an average diameter of 80 nm were used as reinforcement. Fig. 2 shows TEM micrograph of Al₂O₃ nanoparticles. The surface of plates was cleaned by acetone before FSP. According to Fig. 3a, a set of holes of 2 mm diameter and 3 mm depth with 3 mm intervals was made in the middle of the work piece and was then filled with Al₂O₃ nanoparticles as reinforcement phase. The tool was made of H13 tool steel hardened to 52 HRC. A shoulder of 20 mm diameter with a threaded pin diameter of 6 mm and pin length of 3 mm was used for FSP. Fig. 3b shows the threaded tool and its dimensions. All experiments were carried out at room temperature. The tilt angle of the rotating tool with respect to the z-axis of the milling machine was 3° for all samples. The rotational and travel speeds were chosen as 710 rpm and 14 mm/min, respectively.

Table 1. Chemical composition of Al5083 used in this study.

Elements	Zn	Cu	Ti	Si	Cr	Fe	Mn	Mg	Al
Wt%.	0.063	0.04	0.026	0.1	0.1	0.31	0.61	4.27	Bal.

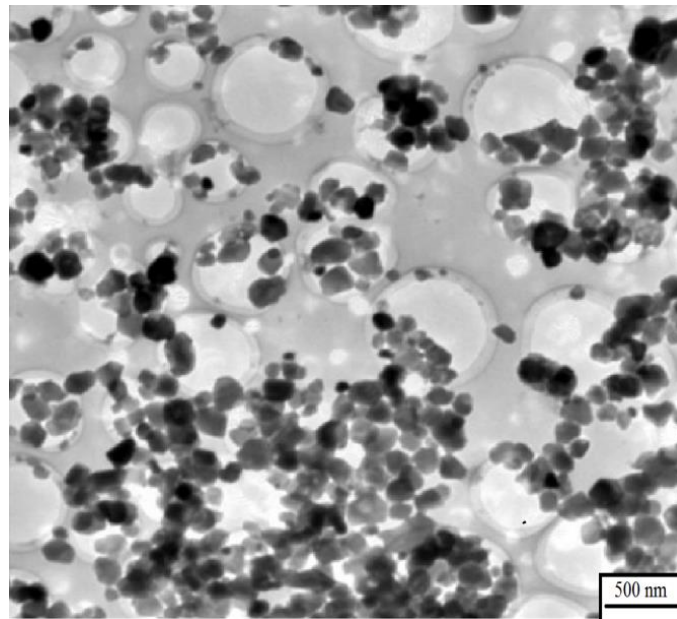


Fig. 2. TEM micrograph of Al₂O₃ nanoparticles.

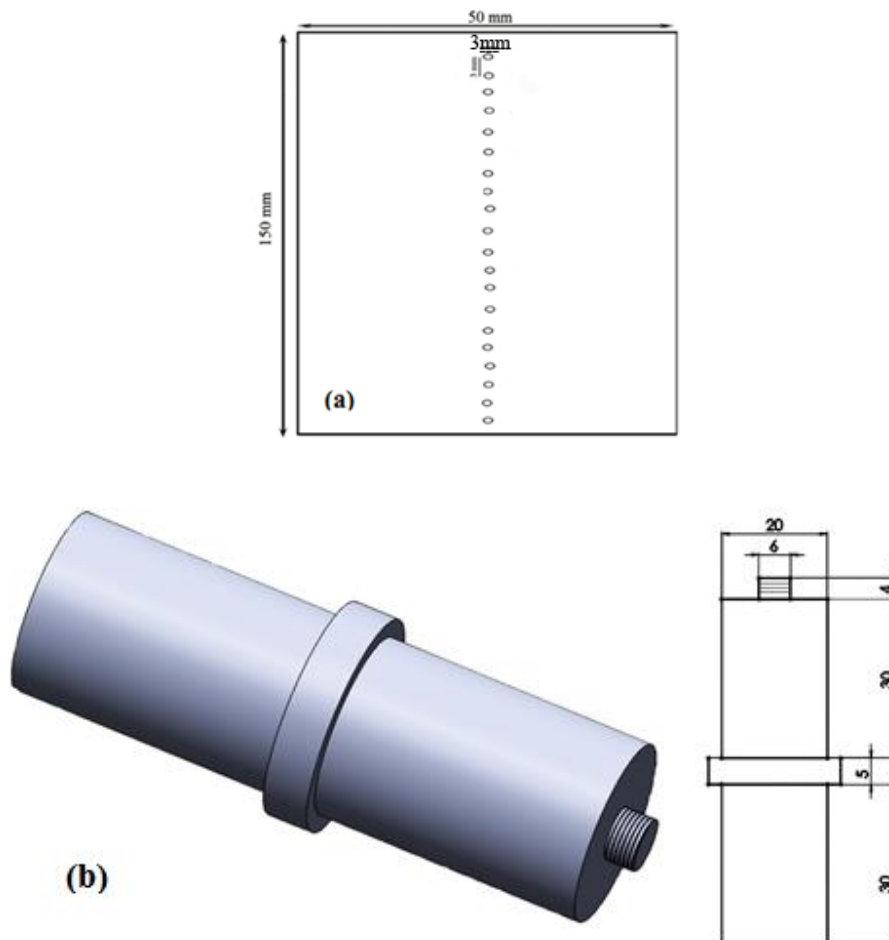


Fig. 3. a) Schematic of Al5083 sheet with the given dimensions and holes with a diameter and depth of 3 mm.
 b) macrograph and dimensions of the FSP tool.

For microstructural characterization, the specimens were prepared according to ASTM E3-01 and then etched for 1 min in modified Poulton's reagent-solution (Table 2). Both scanning electron microscopy (SEM) and optical microscopy (OM) were used to investigate the microstructures. In addition, grain size measurement was carried out by using an image analyzer. The chemical composition of local areas in the specimens was analyzed by an energy dispersive X-ray spectroscopy (EDS) analysis system as an equipment of Jeol SEM.

Table 2. Modified Poulton's reagent-solution.

H ₂ O	CrO ₃	HF	HNO ₃
84 ml	3 g	0.5 ml	15.5 ml

The corresponding mechanical properties of FSP samples were evaluated through microhardness measurements and tensile tests. Tensile specimens were machined to the depth that FSP was applied along the longitudinal direction. Room temperature tensile tests were conducted on the samples as per sub size ASTM E8/E8M-011 via the Santam tensile machine at the strain rate of 0.1 mm/min. Fig. 4 shows the dimensions of the tensile test specimens. The tensile tests were repeated three times for each sample.

Vickers microhardness of the base metal and treated surfaces was measured based on the ASTM-E384 using Buehler's equipment by applying a load of 200 g for 15 seconds.

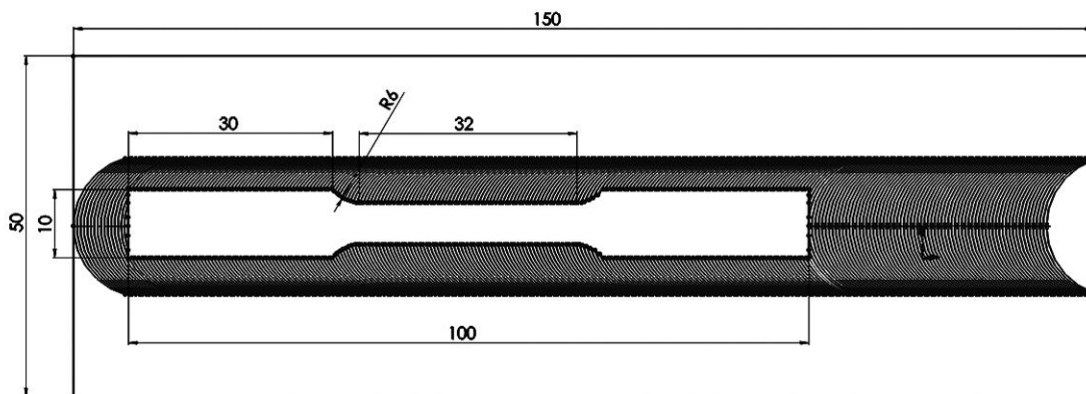


Fig. 4. Schematic illustration of the dimensions of tensile specimen.

The wear behavior of the surface composite layer was studied through pin on disk tribometer (made by Arca Sanat Arvin Co.) at 20°C and humidity of 28%. Wear test specimens of 15 mm diameter were cut from the middle of FSPed surface stir zone. Tribo tests were conducted according to ASTM G99-04 standard. The counterpart discs were made of EN-24 steel hardened to 58 HRC and the surface roughness (Ra) of 0.2 μm. A constant track diameter 100 mm was used in all tests. Before the test, the surface of each pin was polished on 1000 grit emery paper. The wear test was conducted at a sliding velocity of 1 m/s, normal force of 20 N and sliding distance of 500 m. Within every 100 m interval, the samples were cleaned with acetone and weighed to an accuracy of 0.001 mg by electronic weighing balance. The applied load and the sliding speed were fixed in order to

compare the active wear mechanisms in similar conditions. Keeping the sliding velocity and the normal force constant, the friction coefficient between the pin specimen and disc was determined by measuring the frictional force with a stress sensor at the distance of 500 m and without any disc rotation pause. To understand the wear mechanisms, the worn areas of the surface composite layer and base metal were examined by SEM.

3- Results and discussion

3-1- Microstructure

Fig. 5a represents the optical micrograph of the as-received base alloy sample. Figs. 5b, c represent the micrograph of the FSPed alloy without/with Al₂O₃ reinforcement. In this case, a clear grain structure modification and refinement in SZ has occurred. The average

grain size of the as-received base alloy matrix before FSP treatment was 45 μm , which is reduced to 20 μm after FSP. The grain size in the SZ was further reduced to 7 μm by the addition of Al_2O_3 nanoparticles. It indicates that plastic deformation and temperature increasing had been sufficiently high by FSP to cause dynamic recrystallization and grain refinement. In all cases, a good bonding between SZ and TMAZ was attained and no cracks or voids were generated.

SEM micrograph of the cross section of the FSPed samples with Al_2O_3 nanoparticles as well as EDS spectra is shown in Fig. 6. As can be seen in this figure, the particles are homogeneously distributed in the Al matrix. The presence of nano-sized reinforcement particles results in further reduction of the grain size due

to the pinning effect of reinforcements which prevent grain growth. The EDS spectra prove that the second phase is Al_2O_3 .

During friction stir processing, severe increase of temperature and high plastic deformation lead to the formation of a fine equiaxed microstructure in the stir zone. Dynamic recovery (DRV), geometric dynamic recrystallization (GDRX) and discontinuous dynamic recrystallization (DDRX) have been considered as the main mechanisms for grain refinement during FSP [15, 19]. In addition, the presence of reinforcements as second phase promotes grain refinement. These hard particles prevent the grain growth of new recrystallized grains by several mechanisms called the pinning effect [17].

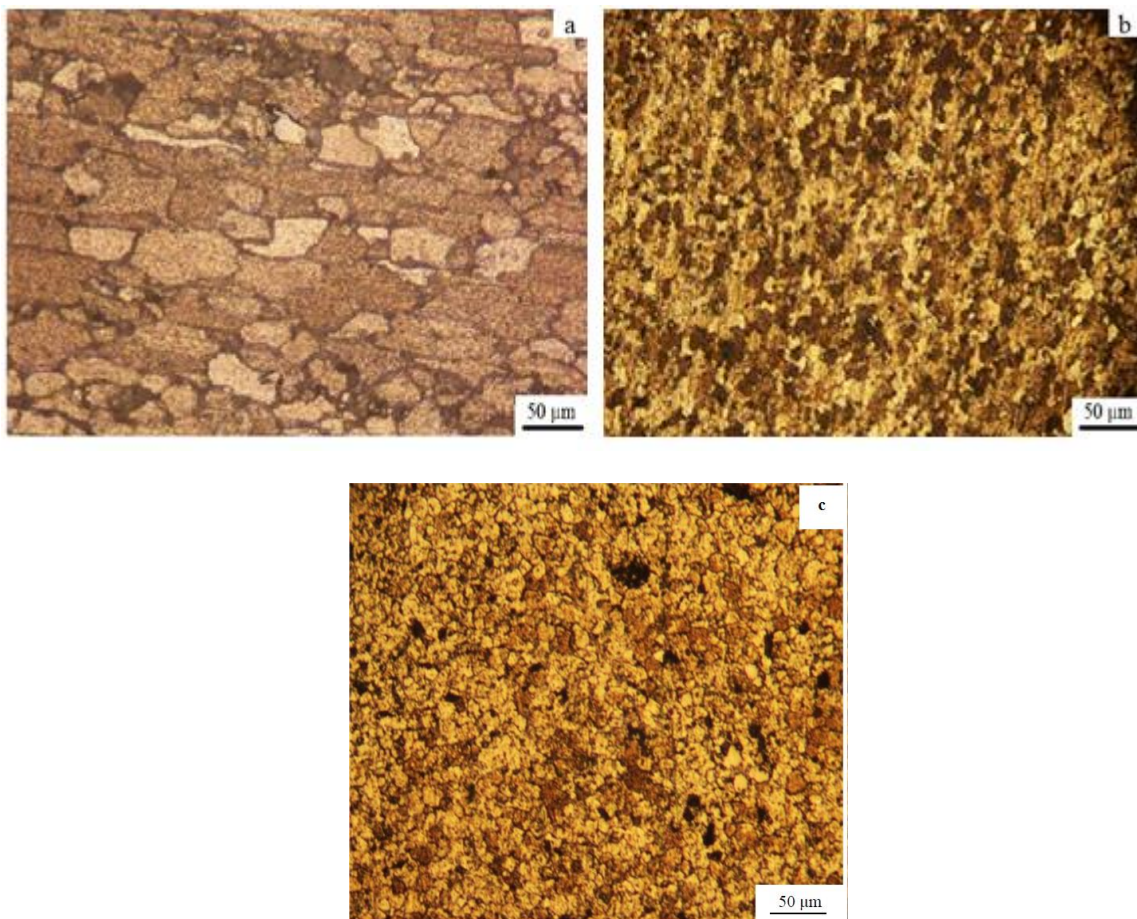


Fig. 5. Optical micrographs of the base alloy Al5083, a) base metal, b) FSPed without reinforcement and c) FSPed with reinforcement.

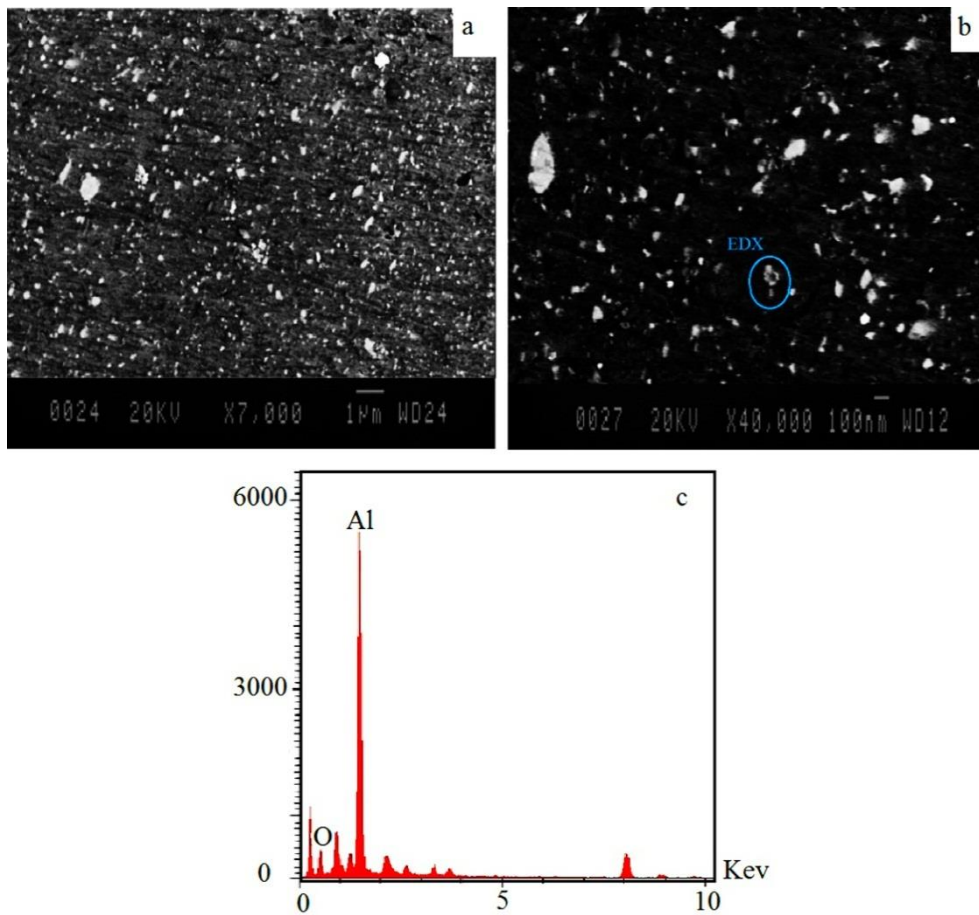


Fig. 6. SEM micrograph of Al5083/Al₂O₃ nanocomposite and the related EDS spectra.

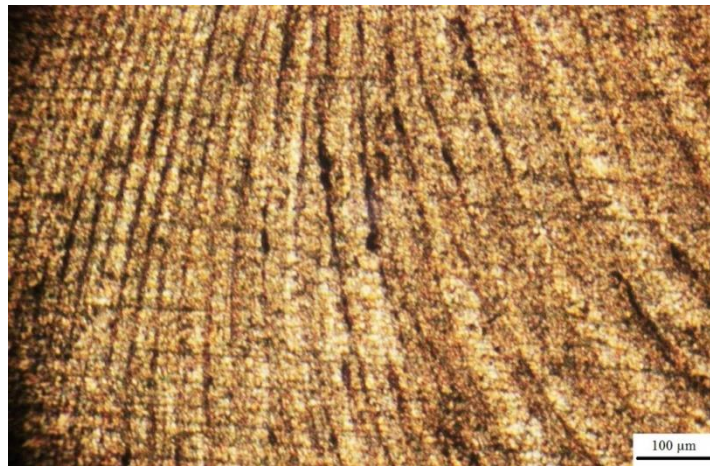


Fig. 7. Micrograph of SZ with onion rings structure.

Another typical microstructural feature in FSP is the appearance of onion rings which is characteristic of material flow. The rings are very close to each other and no island (unmixed regions) is formed between them (Fig. 7), which

is a sign of good material mixing in the SZ. The change of grain size has two main reasons: (1) the heat input, resulting in annealing and grain growth inside SZ; (2) continuous dynamic recrystallization due to FSP that produces new

sites for nucleation, so grains size will decrease in SZ [19].

3-2- Microhardness

Fig. 8 shows the results of microhardness measurement at the surface and cross section of the base metal and Al5083/Al₂O₃ nanocomposite and also the results of microhardness test from cross section of FSPed sample without reinforcement. The average hardness of the as-received 5083 aluminum was 80Hv, which increased to 90 Hv after FSP without Al₂O₃ nanoparticles. In the case of Al₂O₃ nanoparticles addition to the stir zone, the microhardness value increased to about 140 Hv which clearly implies the influence of Al₂O₃ addition on the hardness. In addition, the hardness distribution in the stir zone (SZ) of the FSPed samples is relatively uniform, because the Al₂O₃ nanoparticles distributed uniformly in the matrix are accompanied by further grain size reduction.

In general, the hardness of aluminum alloys can be increased by several methods: solid solution

hardening, grain refinement strengthening, work or strain hardening, and precipitation hardening. During FSP, the changes in hardness for heat treatable (precipitation-hardened) and non-heat-treatable (solid-solution-hardened) aluminum alloys can be different [6]. For the solid solution hardened aluminum, generally FSP does not result in softening the samples; the hardness profile was roughly uniform in the processed zone. However, it was slightly higher than that in the base material. According to the Hall–Petch relationship, with the decrease in grain size, hardness value raises. Consequently, fine grains produced in the FSPed specimen with Al₂O₃ nanoparticles have a positive effect on the hardness value. This effect was also reported by some other researchers [19-22]. Moreover, microhardness increased in the SZ because of the Al₂O₃ nanoparticles which are the harder phase and were distributed uniformly in the aluminum matrix.

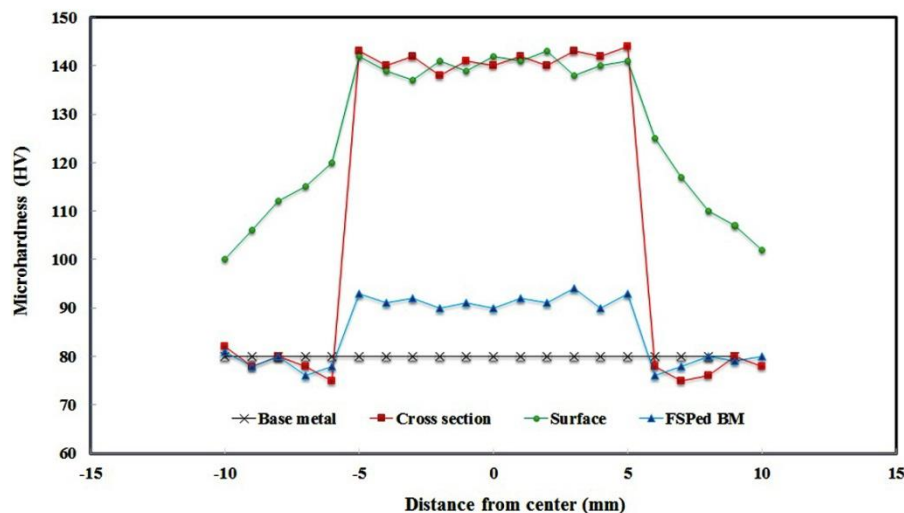


Fig. 8. Microhardness profile from processed region to unprocessed region for the cross section of different samples and for the surface of nanocomposite.

3-3- Tensile test

Fig. 6 shows the stress-strain curves of Al5083 base metal and FSPed specimens with and without Al₂O₃ reinforcement nanoparticles. FSP resulted in a significant improvement in tensile properties. The maximum tensile strength of 335 MPa was achieved for Al5083-Al₂O₃ nanocomposite. It is corresponding to

19.6 % increase in tensile strength of the base alloy. Thus, it can be concluded that the strength of Al5083 base alloy increased when it was subjected to FSP especially with the addition of reinforcement. Although the tensile properties of all FSPed specimens improved, a decrease in elongation from 47 to 21 % was observed. Generally speaking, as the strength of a given

material increased, there is a decrease in its ductility. Also, it is suggested that the reduction

in elongation with the decrease in grain size is an inherent property of materials [6, 10].

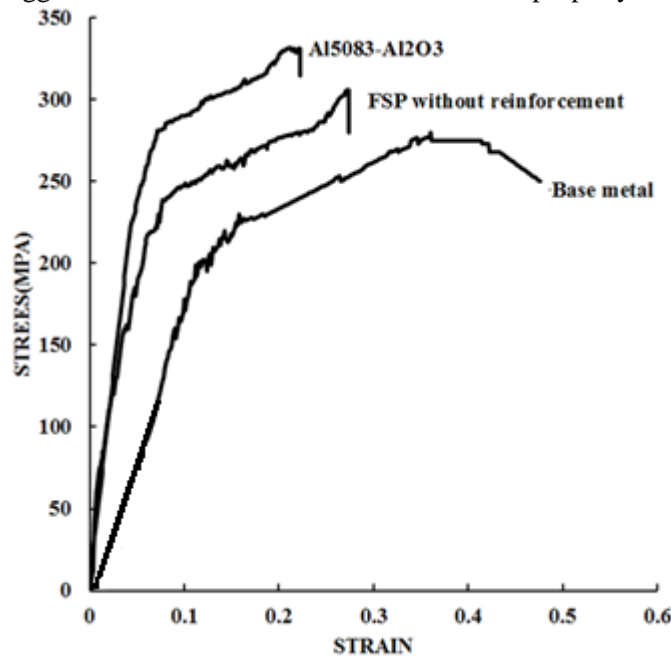


Fig. 9. Stress–strain curves of the tensile tests.

The improvement in mechanical properties of aluminum composites is believed to be due to different mechanisms. The first is the Orowan mechanism [22, 23], where the motion of the dislocations is inhibited by nano sized particles provided that they are closely spaced. The second mechanism is considered to be due to the large coefficient of thermal expansion mismatch between the aluminum matrix and the reinforcements [23], which results in increasing and punching of dislocations at the interface, leading to work hardening of the matrix. The third mechanism is the shear lag mechanism where the load is transferred from the matrix to the reinforcement by interfacial shear stress, provided that there is a good interfacial bonding between the matrix and reinforcement, as recently reported by Bradbury et al. [24] for Al/MWCNTs composites. Liu et al. [25] found the shear lag mechanism very effective in improving the strength of FSPed MWCNTs/Al composites. Additionally, in Al5083 alloy, there are large intermetallic particles such as Al₆(Mn,Fe) which are not dissolved in SZ and get fragmented during FSP [26]. They play the role of fine reinforcement particles when uniformly

distributed in SZ, and can be considered as another strengthening mechanism. In the present study, nano-sized Al₂O₃ particles are distributed in the matrix. On the other hand, grain refinement was achieved in all of the FSPed composites. Of course, there exists a significant mismatch between aluminum matrix and Al₂O₃ particles. Aluminum has a greater coefficient of thermal expansion, i.e. $23.6 \times 10^{-6} \text{ K}^{-1}$, with respect to Al₂O₃ which has a coefficient of thermal expansion of $4.5 \times 10^{-6} \text{ K}^{-1}$. The difference in the coefficients of thermal expansion between the matrix and reinforcing particles, coupled with the temperature change during processing, can create residual plastic strain in the matrix around the particles resulting in generation of dislocation. The dislocation density and its effect on strengthening depend upon reinforcement surface area.

In the present study, it seems that several strengthening effects are simultaneously present. The major mechanisms contributing to the strengthening can be suggested as:

(1) Grain size refinement strengthening due to dynamic recrystallization of FSP and effect of reinforcements on retarding the grain growth.

(2) Orowan strengthening, since reinforcements are in nano scale and uniformly distributed. (3) The dislocation strengthening originating basically from the large coefficient of thermal expansion mismatch between the matrix and the reinforcements.

3-4- Wear properties

To evaluate the wear resistance, Al5083/Al₂O₃ nanocomposite was compared with Al5083 base metal and FSPed specimen without particle (Fig.

10a). Weight loss of the base metal is more than that of the FSPed specimen without particle and Al5083/Al₂O₃ nanocomposite. Wear rates of the as-received Al5083, specimen FSPed without particle and Al5083/Al₂O₃ nanocomposite are presented in Fig. 10b). The wear rate of the as-received Al5083 alloy sample is higher than the FSPed specimen without particle and Al5083/Al₂O₃ nanocomposite.

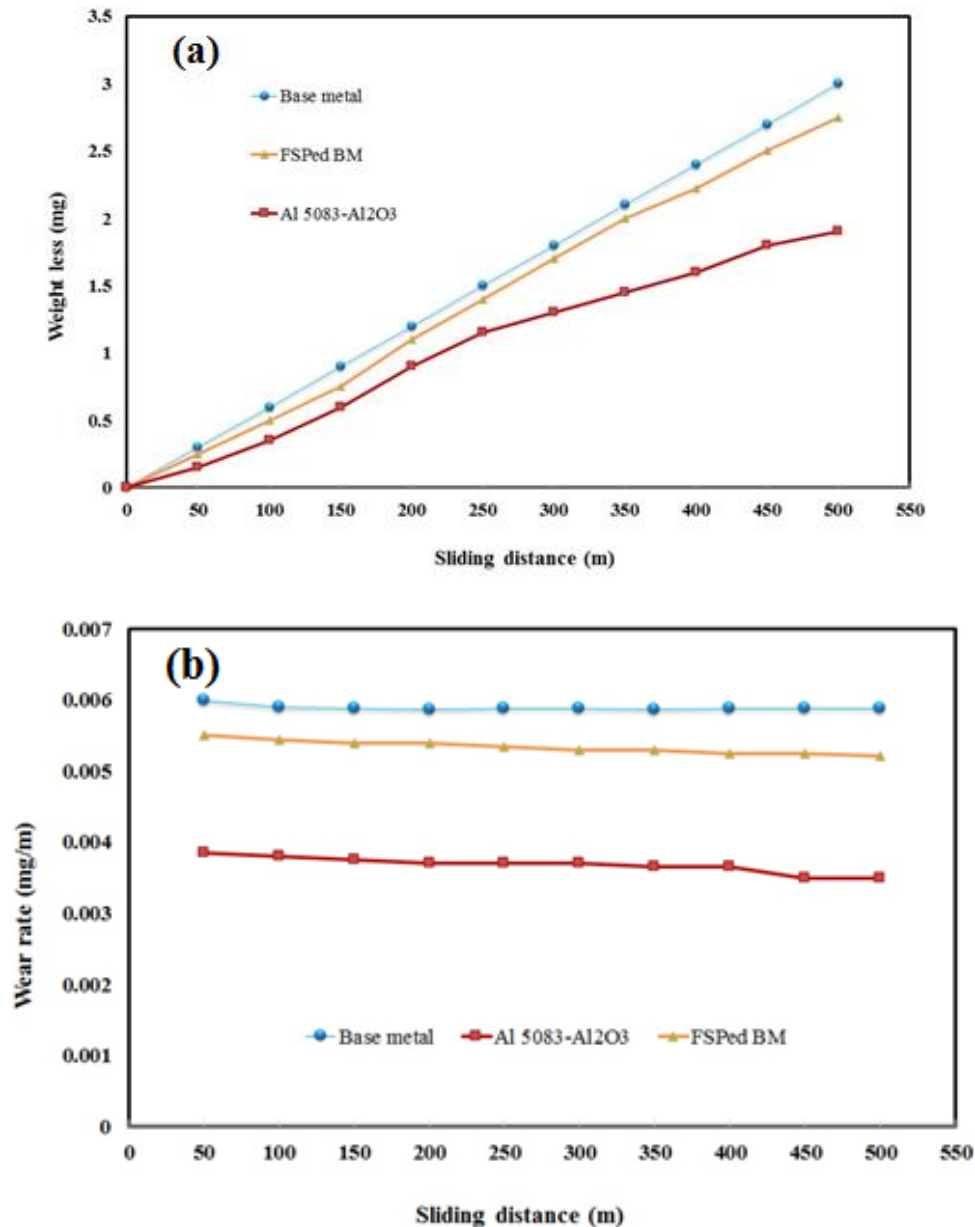


Fig. 10. (a) Weight loss and (b) wear rate vs. distance profiles of the as-received Al5083, FSPed specimen without reinforcement and Al5083/Al₂O₃ nanocomposite.

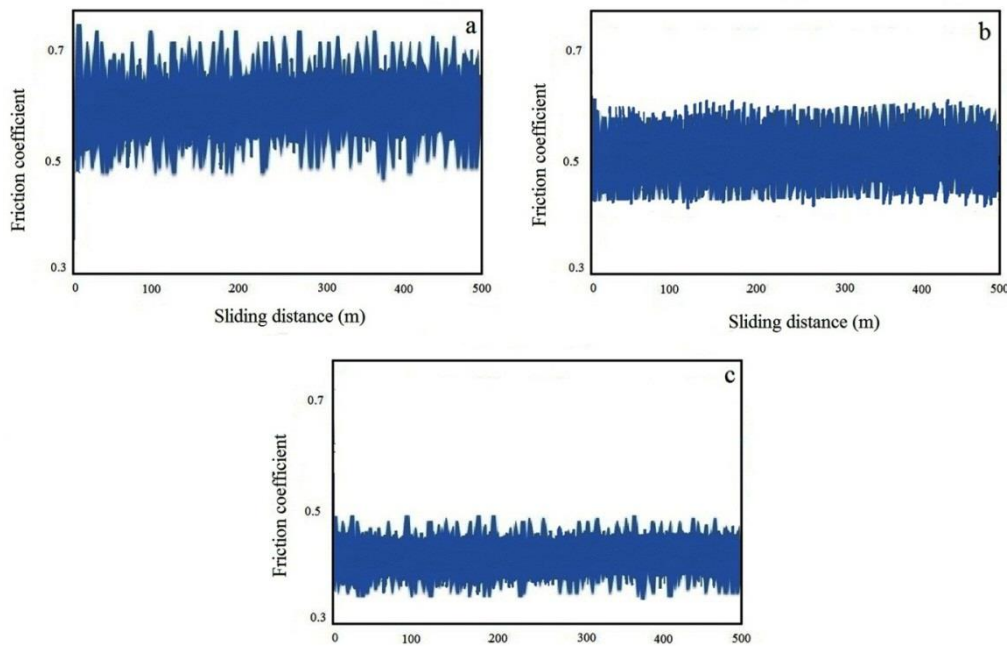


Fig. 11. Variation of friction coefficient vs. distance of (a) as received Al5083 (b) FSPed specimen without reinforcement and (c) Al5083/Al₂O₃ nanocomposite.

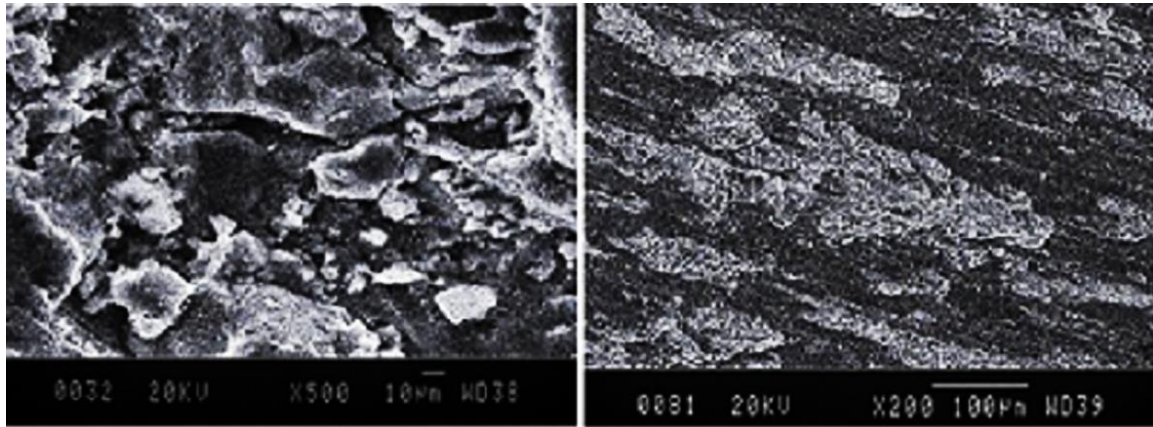
There are several reasons for the enhancement of wear resistance such as:

- 1- Orowan strengthening mechanism because of fine dispersion of Al₂O₃ nanoparticles [27].
- 2- Enhancing microhardness because of Al₂O₃ nanoparticles, and consequently improvement in wear resistance [28].
3. Decreasing the direct load contact between Al5083/Al₂O₃ nanocomposite and pin in comparison with the as-received Al5083 because of dividing the load between Al₂O₃ nanoparticles and Al5083 [28, 29].

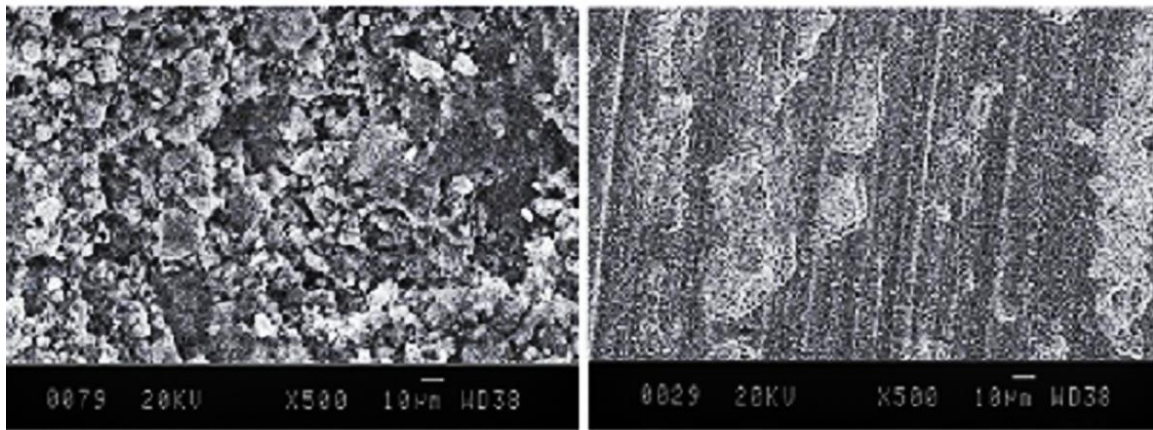
Fig. 11 shows friction coefficient vs. distance of the as-received Al5083, FSPed specimen without particle and Al5083/Al₂O₃ nanocomposite. It can be seen that after a short time a steady state period is sustaining. The friction coefficients of the surface composite are lower and more uniform, in comparison with the base alloy. Lower friction coefficient suggests that the mechanism of wear is chiefly abrasive because of the harder surface scratching over the softer surface. On the other hand, the coefficient of friction was found to be increased to a high value (in some locations) during wearing the samples. Higher friction coefficient is attributed to a localized welding of the worn debris to the sample surface. Averagely, the friction

coefficient in Al5083, FSPed sample without particle and Al5083/Al₂O₃ nanocomposite is 0.61, 0.5 and 0.42, respectively. According to Dolatkah et al. [30] lower friction coefficient in Al5052/SiC composite is due to the presence of reinforcing particles and their obstacle role in the composite which results in higher resistance against surface sliding. According to Figs.10 and 11, friction stir processing leads to the increase of wear resistance and the decrease of the friction coefficient.

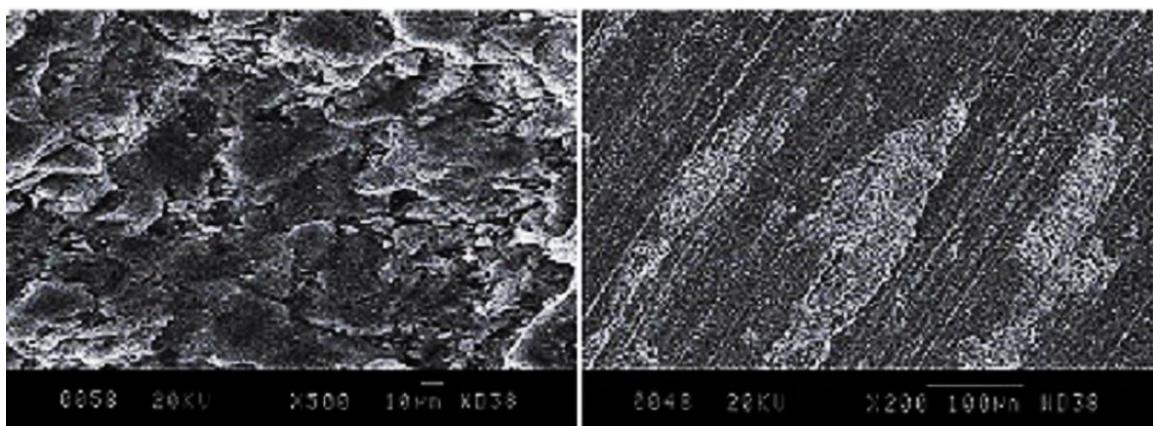
Fig. 12 shows SEM micrograph of the worn surface of the as-received Al5083, FSPed specimen without particle, and Al5083/Al₂O₃ nanocomposite. As can be seen, the fluctuation of Al5083 is more than that of the FSPed sample without particle and Al5083/Al₂O₃ composite probably due to intense cohesion between Al5083 and counterpart [31]. Qu et al. produced Al/Al₂O₃ and Al/SiC composites by FSP and reported that fluctuations of composites are lower than pure Al [32]. It is observed that Al5083/Al₂O₃ nanocomposite exhibits better wear behavior in comparison to Al5083. There are several investigations that confirm this result [12, 30]. In this study, as the FSPed surface was much softer than the pin, the pin could deeply cut and penetrate into the surface, causing severe



(a)



(b)



(c)

Fig. 12. SEM micrograph of the worn surface of (a) as received Al5083, (b) FSPed specimen without reinforcement and (c) Al5083/Al₂O₃ nanocomposite.

plastic deformation of the surface and the material in the contact region undergoes plastic deformation under the combined normal compression and shear stresses. The introduction of a harder reinforcing phase, which is distributed in a ductile matrix with a certain volume fraction, can reduce ductility of the matrix material in the contact region, and the wear of the matrix can be reduced as well. The presence of wear debris and emerging reinforcement agents from nanocomposite, acted as a barrier, leads to abrasive wear mode. This reduces the friction coefficient and improves the wear resistance. Based on the friction coefficient and observation of the microstructure of the worn surfaces, it could be concluded that the improved wear resistance of surface nanocomposite layers is attributed to greater microhardness due to fine dispersion of nanosized particles. The nanoparticles effectively avoided the surface to be penetrated and cut. These nanoparticles are not easily cut out by the pin, because of their small size, high values of hardness, and good bonding with the matrix. In addition, hard ceramic particles such as Al₂O₃ have load bearing behavior [26] and then cause a notable reduction of direct load contact between the matrix and particles, thus wear resistance of surface nanocomposite is improved.

4- Conclusions

In this study, microstructure and properties of Al₅₀₈₃/Al₂O₃ nanocomposite produced by friction stir processing (FSP) were investigated and compared with the as-received Al₅₀₈₃ and FSPed specimen without adding reinforcement. The results showed that designing a net hole on the surface of the base metal was very effective in attaining a uniform distribution of Al₂O₃ nanoparticles and to prevent agglomeration of Al₂O₃ nanoparticles. The stir zone had fine and equiaxed grains of 7 μm due to grain growth inhibiting nature of nanoparticles in the matrix. The maximum tensile strength and hardness value was achieved for Al₅₀₈₃- Al₂O₃ composite due to grain refinement and effective dispersion of nanoparticles. Microhardness and tensile strength of the as-received alloy and surface nanocomposite specimens were about 80 Hv, 280 MPa and 140 Hv and 335 MPa, respectively. Surface nanocomposites revealed

low friction coefficients and wear rates, which were significantly lower than those obtained for the substrate. Scanning electron microscopy tests revealed abrasive wear mechanism on the surface of the wear test specimens.

References

- [1] S. Sharaki, S. Khorasani, R. Abdi, Y. Fotouhi, and H. Bisadi, "Producing of AA5083/ZrO₂ Nanocomposite by Friction Stir Processing (FSP)", *Metal. Mater. Trans. B*, Vol. 44, 2013, pp. 1546-1554.
- [2] R. S. Mishra, M. W. Mahoney, S. X. McFadden, N. A. Mara, A. K. Mukherjee, "High strain rate superplasticity in a friction stir processed 7075 al alloy", *Scripta Mater.*, Vol. 42, 2000, pp. 163-168.
- [3] R. S. Mishra, M. W. Mahoney, "Friction stir processing: a new grain refinement technique to achieve high strain rate superplasticity in commercial alloys", *Mater. Sci. Forum*, Vol. 507, 2001, pp. 357-359.
- [4] R. S. Mishra, Z. Y. Ma, I. Charit, "Friction stir processing: a novel technique for fabrication of surface composite", *Mater. Sci. Eng. A*, Vol. 341, 2003, pp. 307-310.
- [5] M. Narimani, B. Lotfi, Z. Sadeghian, "Investigating the effect of tool dimension and rotational speed on microstructure of Al-B4C surface composite layer produced by friction stir processing (FSP)", *J. Adv. Mater. Proc.* Vol.3, No.2, 2015, pp.61-70
- [6] R. S. Mishra, Z. Y. Ma, "Friction stir welding and processing", *Mater. Sci. Eng. R*, Vol. 50, 2005, pp. 1-78.
- [7] Z. Y. Ma, S. R. Sharma, R. S. Mishra, M. W. Manohey, "Microstructural modification of cast Aluminum alloys via friction stir processing", *Mater. Sci. Forum*, Vol. 426-432, 2003, pp. 2891- 2896.
- [8] C. M. Hu, C. M. Lai, X. H. Du, N. J. Ho, J. C. Huang, "Enhanced tensile plasticity in ultrafinegrained metallic composite fabricated by friction stir process", *Scripta Mater.*, Vol. 59, 2008, pp. 1163-1166.
- [9] Q. Liu, L. Ke, F. Liu, C. Huang, L. Xing, "Microstructure and mechanical property of multiwalled carbon nanotubes reinforced aluminum matrix composites fabricated by friction stir processing", *Mater. Des.*, Vol. 45, 2013, pp. 343-348.

- [10] R. Kapoor, K. Kandasamy, R. S. Mishra, J. A. Baumann, G. Grant, "Effect of friction stir processing on the tensile and fatigue behavior of a cast A206 alloy", *Mater. Sci. Eng. A*, Vol. 561, 2013, pp. 159–166.
- [11] S. Jana, R. S. Mishra, J. B. Baumann, G. Grant, "Effect of friction stir processing on fatigue behavior of an investment cast Al–7Si–0.6 Mg alloy", *Acta Mater.*, Vol. 58, pp. 989–1003, (2010).
- [12] S. Soleymani, A. Abdollah-zadeh, S. A. Alidokht, "Microstructural and tribological properties of Al5083 based surface hybrid composite produced by friction stir processing", *Wear*, Vol. 278–279, 2012, pp. 41–47.
- [13] A. Shafiei-Zarghani, S. F. Kashani-Bozorg, A. Zarei-Hanzaki, "Wear assessment of Al/Al₂O₃ nano-composite surface layer produced using friction stir processing", *Wear*, Vol. 270, 2011, pp. 403–412.
- [14] K. Surekha, B. S. Murty, K. Prasad Rao, "Effect of processing parameters on the corrosion behavior of friction stir processed AA 2219 aluminum alloy", *Solid Stat. Sci.*, Vol. 11, 2009, pp. 907–917.
- [15] C. J. Hsu, P. W. Kao, N. J. Ho, "Ultrafine-grained Al–Al₂Cu composite produced in situ by friction stir processing", *Scripta Mater.*, Vol. 53, 2005, pp. 341–345.
- [16] Y. Mazaheri, F. Karimzadeh, M. H. Enayati, "A novel technique for development of A356/Al₂O₃ surface nanocomposite by friction stir processing", *J. Mater. Proc. Tech.*, Vol. 211, 2011, pp. 1614–1619.
- [17] K. J. Hodder, H. Izadi, A. G. McDonald, A. P. Gerlich, "Fabrication of aluminum-alumina metal matrix composites via cold gas dynamic spraying at low pressure followed by friction stir processing", *Mater. Sci. Eng. A*, Vol. 556, 2012, pp. 114–121.
- [18] H. R. Akramifard, M. Shamanian, M. Sabbaghian, M. Esmailzadeh, "Microstructure and mechanical properties of Cu/SiC metal matrix composite fabricated via friction stir processing", *Mater. Des.*, Vol. 54, 2014, pp. 838–844.
- [19] M. Barmouz, M. K. B. Givi, J. Seyfi, "On the role of processing parameters in producing Cu/SiC metal matrix composites via friction stir processing: Investigating microstructure, microhardness, wear and tensile behavior", *Mater. Charac.*, Vol. 62, 2011, pp. 108–117.
- [20] J. A. Schneider, A. C. Nunes, "Characterization of plastic flow and resulting micro textures in a friction stir weld", *Mater. Trans. B*, Vol. 35, 2004, pp. 777–783.
- [21] Y. F. Sun, H. Fujii, "The effect of SiC particles on the microstructure and mechanical properties of friction stir welded pure copper joints", *Mater. Sci. Eng. A*, Vol. 528, 2011, pp. 5470–5475.
- [22] Z. Zhang, D. L. Chen, "Contribution of Orowan strengthening effect in particulate reinforced metal matrix nanocomposites", *Mater. Sci. Eng. A*, Vol. 483–484, 2008, pp. 148–152.
- [23] R. George, K. T. Kashyap, R. Rahul, S. Yamdagni, "Strengthening in carbon nanotube/aluminum (CNT/Al) composites", *Scripta Mater.*, Vol. 53, 2005, pp. 1159–1163.
- [24] C. R. Bradbury, J. K. Gomon, L. Kollo, H. Kwon, M. Leparoux, "Hardness of Multi Wall Carbon Nanotubes reinforced aluminum matrix composites", *J. Alloy. Comp.*, Vol. 585, 2014, p. 362–367.
- [25] Q. Liu, L. Ke, F. Liu, C. Huang, L. Xing, "Microstructure and mechanical property of multiwalled carbon nanotubes reinforced aluminum matrix composites fabricated by friction stir processing", *Mater. Des.*, Vol. 45, 2013, pp. 343–348.
- [26] C. Y. Lin, T. S. Lui, L. H. Chen, "Microstructural variation and tensile properties of a cast 5083 aluminum plate via friction stir processing", *Mater. Trans.*, Vol. 50, 2009, pp. 2801–2807.
- [27] C. Maxwell Rejil, I. Dinaharan, S. J. Vijay, N. Murugan, "Microstructure and sliding wear behavior of AA6360/(TiC+B₄C) hybrid surface composite layer synthesized by friction stir processing on aluminum substrate", *Mater. Sci. Eng. A*, Vol. 552, 2012, pp. 336–344.
- [28] C. S. Ramesh, R. NoorAhmed, M. A. Mujeebu, M. Z. Abdullah, "Development and performance analysis of novel cast copper–SiC–Gr hybrid composites", *Mater. Des.*, Vol. 30, 2009, pp. 1957–1965.
- [29] E. R. I. Mahmoud, M. Takahashi, T. Shibayanagi, K. Ikeuchi, "Wear characteristics of surface-hybrid-MMCs layer fabricated on aluminum plate by friction stir processing", *Wear*, Vol. 268, 2010, pp. 1111–1121.
- [30] A. Dolatkah, P. Golbabaei, M. K. B. Givi, F. Molaiekiya, "Investigating effects of process

parameters on microstructural and mechanical properties of Al5052/SiC metal matrix composite fabricated via friction stir processing”, *Mater. Des.*, Vol. 37, 2012, pp. 458-464.

[31] Q. Zhang, B. L. Xiao, W. G. Wang, Z. Y. Ma, “Reactive mechanism and mechanical properties of in situ composites fabricated from an Al-TiO₂ system by friction stir processing”, *Acta Mater.*, Vol. 60, 2012, pp. 7090-7103.

[32] J. Qu, H. Xu, Z. Feng, D. A. Frederick, L. An, H. Heinrich, “Improving the tribological characteristics of aluminum 6061 alloy by surface compositing with submicro-size ceramic particles via friction stir processing”, *Wear*, Vol. 271, 2011, pp. 1940–1945.